Evidence for tt[over ¯]γ production and measurement of σ_{tt[over ¯]γ}/σ_{tt[over ¯]}

T. Aaltonen *et al.* (CDF Collaboration)

Evidence for $t\bar{t}\gamma$ Production and Measurement of $\sigma_{t\bar{t}\gamma}/\sigma_{t\bar{t}}$

T. Aaltonen,[21] B. Álvarez González[v],[9] S. Amerio,[41] D. Amidei,[32] A. Anastassov,[36] A. Annovi,[17] J. Antos,[12] G. Apollinari,[15] J.A. Appel,[15] A. Apresyan,[46] T. Arisawa,[56] A. Artikov,[13] J. Asaadi,[51] W. Ashmanskas,[15] B. Auerbach,[59] A. Aurisano,[51] F. Azfar,[40] W. Badgett,[15] A. Barbaro-Galtieri,[26] V.E. Barnes,[46] B.A. Barnett,[23] P. Barria[cc],[44] P. Bartos,[12] M. Bauce[aa],[41] G. Bauer,[30] F. Bedeschi,[44] D. Beecher,[28] S. Behari,[23] G. Bellettini[bb],[44] J. Bellinger,[58] D. Benjamin,[14] A. Beretvas,[15] A. Bhatti,[48] M. Binkley[*],[15] D. Bisello[aa],[41] I. Bizjak[gg],[28] K.R. Bland,[5] B. Blumenfeld,[23] A. Bocci,[14] A. Bodek,[47] D. Bortoletto,[46] J. Boudreau,[45] A. Boveia,[11] B. Brau[a],[15] L. Brigliadori[z],[6] A. Brisuda,[12] C. Bromberg,[33] E. Brucken,[21] M. Bucciantonio[bb],[44] J. Budagov,[13] H.S. Budd,[47] S. Budd,[22] K. Burkett,[15] G. Busetto[aa],[41] P. Bussey,[19] A. Buzatu,[31] C. Calancha,[29] S. Camarda,[4] M. Campanelli,[33] M. Campbell,[32] F. Canelli[12],[15] A. Canepa,[43] B. Carls,[22] D. Carlsmith,[58] R. Carosi,[44] S. Carrillo[k],[16] S. Carron,[15] B. Casal,[9] M. Casarsa,[15] A. Castro[z],[6] P. Catastini,[15] D. Cauz,[52] V. Cavaliere[cc],[44] M. Cavalli-Sforza,[4] A. Cerri[f],[26] L. Cerrito[q],[28] Y.C. Chen,[1] M. Chertok,[7] G. Chiarelli,[44] G. Chlachidze,[15] F. Chlebana,[15] K. Cho,[25] D. Chokheli,[13] J.P. Chou,[20] W.H. Chung,[58] Y.S. Chung,[47] C.I. Ciobanu,[42] M.A. Ciocci[cc],[44] A. Clark,[18] G. Compostella[aa],[41] M.E. Convery,[15] J. Conway,[7] M.Corbo,[42] M. Cordelli,[17] C.A. Cox,[7] D.J. Cox,[7] F. Crescioli[bb],[44] C. Cuenca Almenar,[59] J. Cuevas[v],[9] R. Culbertson,[15] D. Dagenhart,[15] N. d'Ascenzo[t],[42] M. Datta,[15] P. de Barbaro,[47] S. De Cecco,[49] G. De Lorenzo,[4] M. Dell'Orso[bb],[44] C. Deluca,[4] L. Demortier,[48] J. Deng[c],[14] M. Deninno,[6] F. Devoto,[21] M. d'Errico[aa],[41] A. Di Canto[bb],[44] B. Di Ruzza,[44] J.R. Dittmann,[5] M. D'Onofrio,[27] S. Donati[bb],[44] P. Dong,[15] M. Dorigo,[52] T. Dorigo,[41] K. Ebina,[56] A. Elagin,[51] A. Eppig,[32] R. Erbacher,[7] D. Errede,[22] S. Errede,[22] N. Ershaidat[y],[42] R. Eusebi,[51] H.C. Fang,[26] S. Farrington,[40] M. Feindt,[24] J.P. Fernandez,[29] C. Ferrazza[dd],[44] R. Field,[16] G. Flanagan[r],[46] R. Forrest,[7] M.J. Frank,[5] M. Franklin,[20] J.C. Freeman,[15] Y. Funakoshi,[56] I. Furic,[16] M. Gallinaro,[48] J. Galyardt,[10] J.E. Garcia,[18] A.F. Garfinkel,[46] P. Garosi[cc],[44] H. Gerberich,[22] E. Gerchtein,[15] S. Giagu[ee],[49] V. Giakoumopoulou,[3] P. Giannetti,[44] K. Gibson,[45] C.M. Ginsburg,[15] N. Giokaris,[3] P. Giromini,[17] M. Giunta,[44] G. Giurgiu,[23] V. Glagolev,[13] D. Glenzinski,[15] M. Gold,[35] D. Goldin,[51] N. Goldschmidt,[16] A. Golossanov,[15] G. Gomez,[9] G. Gomez-Ceballos,[30] M. Goncharov,[30] O. González,[29] I. Gorelov,[35] A.T. Goshaw,[14] K. Goulianos,[48] A. Gresele,[41] S. Grinstein,[4] C. Grosso-Pilcher,[11] R.C. Group,[55] J. Guimaraes da Costa,[20] Z. Gunay-Unalan,[33] C. Haber,[26] S.R. Hahn,[15] E. Halkiadakis,[50] A. Hamaguchi,[39] J.Y. Han,[47] F. Happacher,[17] K. Hara,[53] D. Hare,[50] M. Hare,[54] R.F. Harr,[57] K. Hatakeyama,[5] C. Hays,[40] M. Heck,[24] J. Heinrich,[43] M. Herndon,[58] S. Hewamanage,[5] D. Hidas,[50] A. Hocker,[15] W. Hopkins[g],[15] D. Horn,[24] S. Hou,[1] R.E. Hughes,[37] M. Hurwitz,[11] U. Husemann,[59] N. Hussain,[31] M. Hussein,[33] J. Huston,[33] G. Introzzi,[44] M. Iori[ee],[49] A. Ivanov[o],[7] E. James,[15] D. Jang,[10] B. Jayatilaka,[14] E.J. Jeon,[25] M.K. Jha,[6] S. Jindariani,[15] W. Johnson,[7] M. Jones,[46] K.K. Joo,[25] S.Y. Jun,[10] T.R. Junk,[15] T. Kamon,[51] P.E. Karchin,[57] Y. Kato[n],[39] W. Ketchum,[11] J. Keung,[43] V. Khotilovich,[51] B. Kilminster,[15] D.H. Kim,[25] H.S. Kim,[25] H.W. Kim,[25] J.E. Kim,[25] M.J. Kim,[17] S.B. Kim,[25] S.H. Kim,[53] Y.K. Kim,[11] N. Kimura,[56] M. Kirby,[15] S. Klimenko,[16] K. Kondo,[56] D.J. Kong,[25] J. Konigsberg,[16] A.V. Kotwal,[14] M. Kreps,[24] J. Kroll,[43] D. Krop,[11] N. Krumnack[l],[5] M. Kruse,[14] V. Krutelyov[d],[51] T. Kuhr,[24] M. Kurata,[53] S. Kwang,[11] A.T. Laasanen,[46] S. Lami,[44] S. Lammel,[15] M. Lancaster,[28] R.L. Lander,[7] K. Lannon[u],[37] A. Lath,[50] G. Latino[cc],[44] I. Lazzizzera,[41] T. LeCompte,[2] E. Lee,[51] H.S. Lee,[11] J.S. Lee,[25] S.W. Lee[w],[51] S. Leo[bb],[44] S. Leone,[44] J.D. Lewis,[15] C.-J. Lin,[26] J. Linacre,[40] M. Lindgren,[15] E. Lipeles,[43] A. Lister,[18] D.O. Litvintsev,[15] C. Liu,[45] Q. Liu,[46] T. Liu,[15] S. Lockwitz,[59] N.S. Lockyer,[43] A. Loginov,[59] D. Lucchesi[aa],[41] J. Lueck,[24] P. Lujan,[26] P. Lukens,[15] G. Lungu,[48] J. Lys,[26] R. Lysak,[12] R. Madrak,[15] K. Maeshima,[15] K. Makhoul,[30] P. Maksimovic,[23] S. Malik,[48] G. Manca[b],[27] A. Manousakis-Katsikakis,[3] F. Margaroli,[46] C. Marino,[24] M. Martínez,[4] R. Martínez-Ballarín,[29] P. Mastrandrea,[49] M. Mathis,[23] M.E. Mattson,[57] P. Mazzanti,[6] K.S. McFarland,[47] P. McIntyre,[51] R. McNulty[i],[27] A. Mehta,[27] P. Mehtala,[21] A. Menzione,[44] C. Mesropian,[48] T. Miao,[15] D. Mietlicki,[32] A. Mitra,[1] H. Miyake,[53] S. Moed,[20] N. Moggi,[6] M.N. Mondragon[k],[15] C.S. Moon,[25] R. Moore,[15] M.J. Morello,[15] J. Morlock,[24] P. Movilla Fernandez,[15] A. Mukherjee,[15] Th. Muller,[24] P. Murat,[15] M. Mussini[z],[6] J. Nachtman[m],[15] Y. Nagai,[53] J. Naganoma,[56] I. Nakano,[38] A. Napier,[54] J. Nett,[51] C. Neu,[55] M.S. Neubauer,[22] J. Nielsen[e],[26] L. Nodulman,[2] O. Norniella,[22] E. Nurse,[28] L. Oakes,[40] S.H. Oh,[14] Y.D. Oh,[25] I. Oksuzian,[55] T. Okusawa,[39] R. Orava,[21] L. Ortolan,[4] S. Pagan Griso[aa],[41] C. Pagliarone,[52] E. Palencia[f],[9] V. Papadimitriou,[15] A.A. Paramonov,[2] J. Patrick,[15] G. Pauletta[ff],[52] M. Paulini,[10] C. Paus,[30] D.E. Pellett,[7] A. Penzo,[52] T.J. Phillips,[14] G. Piacentino,[44] E. Pianori,[43] J. Pilot,[37] K. Pitts,[22] C. Plager,[8] L. Pondrom,[58] K. Potamianos,[46] O. Poukhov[*],[13] F. Prokoshin[x],[13] A. Pronko,[15] F. Ptohos[h],[17] E. Pueschel,[10] G. Punzi[bb],[44] J. Pursley,[58] A. Rahaman,[45] V. Ramakrishnan,[58] N. Ranjan,[46] I. Redondo,[29] P. Renton,[40] M. Rescigno,[49] F. Rimondi[z],[6] L. Ristori[45],[15] A. Robson,[19] T. Rodrigo,[9] T. Rodriguez,[43] E. Rogers,[22] S. Rolli,[54] R. Roser,[15] M. Rossi,[52] F. Rubbo,[15] F. Ruffini[cc],[44]

A. Ruiz,[9] J. Russ,[10] V. Rusu,[15] A. Safonov,[51] W.K. Sakumoto,[47] Y. Sakurai,[56] L. Santi[ff],[52] L. Sartori,[44] K. Sato,[53] V. Saveliev[t],[42] A. Savoy-Navarro,[42] P. Schlabach,[15] A. Schmidt,[24] E.E. Schmidt,[15] M.P. Schmidt*,[59] M. Schmitt,[36] T. Schwarz,[7] L. Scodellaro,[9] A. Scribano[cc],[44] F. Scuri,[44] A. Sedov,[46] S. Seidel,[35] Y. Seiya,[39] A. Semenov,[13] F. Sforza[bb],[44] A. Sfyrla,[22] S.Z. Shalhout,[7] T. Shears,[27] P.F. Shepard,[45] M. Shimojima[s],[53] S. Shiraishi,[11] M. Shochet,[11] I. Shreyber,[34] A. Simonenko,[13] P. Sinervo,[31] A. Sissakian*,[13] K. Sliwa,[54] J.R. Smith,[7] F.D. Snider,[15] A. Soha,[15] S. Somalwar,[50] V. Sorin,[4] P. Squillacioti,[15] M. Stancari,[15] M. Stanitzki,[59] R. St. Denis,[19] B. Stelzer,[31] O. Stelzer-Chilton,[31] D. Stentz,[36] J. Strologas,[35] G.L. Strycker,[32] Y. Sudo,[53] A. Sukhanov,[16] I. Suslov,[13] K. Takemasa,[53] Y. Takeuchi,[53] J. Tang,[11] M. Tecchio,[32] P.K. Teng,[1] J. Thom[g],[15] J. Thome,[10] G.A. Thompson,[22] E. Thomson,[43] P. Tipton,[59] P. Ttito-Guzmán,[29] S. Tkaczyk,[15] D. Toback,[51] S. Tokar,[12] K. Tollefson,[33] T. Tomura,[53] D. Tonelli,[15] S. Torre,[17] D. Torretta,[15] P. Totaro[ff],[52] M. Trovato[dd],[44] Y. Tu,[43] F. Ukegawa,[53] S. Uozumi,[25] A. Varganov,[32] F. Vázquez[k],[16] G. Velev,[15] C. Vellidis,[3] M. Vidal,[29] I. Vila,[9] R. Vilar,[9] J. Vizán,[9] M. Vogel,[35] G. Volpi[bb],[44] P. Wagner,[43] R.L. Wagner,[15] T. Wakisaka,[39] R. Wallny,[8] S.M. Wang,[1] A. Warburton,[31] D. Waters,[28] M. Weinberger,[51] W.C. Wester III,[15] B. Whitehouse,[54] D. Whiteson[c],[43] A.B. Wicklund,[2] E. Wicklund,[15] S. Wilbur,[11] F. Wick,[24] H.H. Williams,[43] J.S. Wilson,[37] P. Wilson,[15] B.L. Winer,[37] P. Wittich[g],[15] S. Wolbers,[15] H. Wolfe,[37] T. Wright,[32] X. Wu,[18] Z. Wu,[5] K. Yamamoto,[39] J. Yamaoka,[14] T. Yang,[15] U.K. Yang[p],[11] Y.C. Yang,[25] W.-M. Yao,[26] G.P. Yeh,[15] K. Yi[m],[15] J. Yoh,[15] K. Yorita,[56] T. Yoshida[j],[39] G.B. Yu,[14] I. Yu,[25] S.S. Yu,[15] J.C. Yun,[15] A. Zanetti,[52] Y. Zeng,[14] and S. Zucchelli[z][6]

(CDF Collaboration†)

[1]*Institute of Physics, Academia Sinica, Taipei, Taiwan 11529, Republic of China*
[2]*Argonne National Laboratory, Argonne, Illinois 60439, USA*
[3]*University of Athens, 157 71 Athens, Greece*
[4]*Institut de Fisica d'Altes Energies, ICREA, Universitat Autonoma de Barcelona, E-08193, Bellaterra (Barcelona), Spain*
[5]*Baylor University, Waco, Texas 76798, USA*
[6]*Istituto Nazionale di Fisica Nucleare Bologna, [z]University of Bologna, I-40127 Bologna, Italy*
[7]*University of California, Davis, Davis, California 95616, USA*
[8]*University of California, Los Angeles, Los Angeles, California 90024, USA*
[9]*Instituto de Fisica de Cantabria, CSIC-University of Cantabria, 39005 Santander, Spain*
[10]*Carnegie Mellon University, Pittsburgh, Pennsylvania 15213, USA*
[11]*Enrico Fermi Institute, University of Chicago, Chicago, Illinois 60637, USA*
[12]*Comenius University, 842 48 Bratislava, Slovakia; Institute of Experimental Physics, 040 01 Kosice, Slovakia*
[13]*Joint Institute for Nuclear Research, RU-141980 Dubna, Russia*
[14]*Duke University, Durham, North Carolina 27708, USA*
[15]*Fermi National Accelerator Laboratory, Batavia, Illinois 60510, USA*
[16]*University of Florida, Gainesville, Florida 32611, USA*
[17]*Laboratori Nazionali di Frascati, Istituto Nazionale di Fisica Nucleare, I-00044 Frascati, Italy*
[18]*University of Geneva, CH-1211 Geneva 4, Switzerland*
[19]*Glasgow University, Glasgow G12 8QQ, United Kingdom*
[20]*Harvard University, Cambridge, Massachusetts 02138, USA*
[21]*Division of High Energy Physics, Department of Physics,*
University of Helsinki and Helsinki Institute of Physics, FIN-00014, Helsinki, Finland
[22]*University of Illinois, Urbana, Illinois 61801, USA*
[23]*The Johns Hopkins University, Baltimore, Maryland 21218, USA*
[24]*Institut für Experimentelle Kernphysik, Karlsruhe Institute of Technology, D-76131 Karlsruhe, Germany*
[25]*Center for High Energy Physics: Kyungpook National University,*
Daegu 702-701, Korea; Seoul National University, Seoul 151-742,
Korea; Sungkyunkwan University, Suwon 440-746,
Korea; Korea Institute of Science and Technology Information,
Daejeon 305-806, Korea; Chonnam National University, Gwangju 500-757,
Korea; Chonbuk National University, Jeonju 561-756, Korea
[26]*Ernest Orlando Lawrence Berkeley National Laboratory, Berkeley, California 94720, USA*
[27]*University of Liverpool, Liverpool L69 7ZE, United Kingdom*
[28]*University College London, London WC1E 6BT, United Kingdom*
[29]*Centro de Investigaciones Energeticas Medioambientales y Tecnologicas, E-28040 Madrid, Spain*
[30]*Massachusetts Institute of Technology, Cambridge, Massachusetts 02139, USA*
[31]*Institute of Particle Physics: McGill University, Montréal, Québec,*
Canada H3A 2T8; Simon Fraser University, Burnaby, British Columbia,
Canada V5A 1S6; University of Toronto, Toronto, Ontario,
Canada M5S 1A7; and TRIUMF, Vancouver, British Columbia, Canada V6T 2A3
[32]*University of Michigan, Ann Arbor, Michigan 48109, USA*
[33]*Michigan State University, East Lansing, Michigan 48824, USA*

[34]Institution for Theoretical and Experimental Physics, ITEP, Moscow 117259, Russia
[35]University of New Mexico, Albuquerque, New Mexico 87131, USA
[36]Northwestern University, Evanston, Illinois 60208, USA
[37]The Ohio State University, Columbus, Ohio 43210, USA
[38]Okayama University, Okayama 700-8530, Japan
[39]Osaka City University, Osaka 588, Japan
[40]University of Oxford, Oxford OX1 3RH, United Kingdom
[41]Istituto Nazionale di Fisica Nucleare, Sezione di Padova-Trento, [aa]University of Padova, I-35131 Padova, Italy
[42]LPNHE, Universite Pierre et Marie Curie/IN2P3-CNRS, UMR7585, Paris, F-75252 France
[43]University of Pennsylvania, Philadelphia, Pennsylvania 19104, USA
[44]Istituto Nazionale di Fisica Nucleare Pisa, [bb]University of Pisa,
[cc]University of Siena and [dd]Scuola Normale Superiore, I-56127 Pisa, Italy
[45]University of Pittsburgh, Pittsburgh, Pennsylvania 15260, USA
[46]Purdue University, West Lafayette, Indiana 47907, USA
[47]University of Rochester, Rochester, New York 14627, USA
[48]The Rockefeller University, New York, New York 10065, USA
[49]Istituto Nazionale di Fisica Nucleare, Sezione di Roma 1,
[ee]Sapienza Università di Roma, I-00185 Roma, Italy
[50]Rutgers University, Piscataway, New Jersey 08855, USA
[51]Texas A&M University, College Station, Texas 77843, USA
[52]Istituto Nazionale di Fisica Nucleare Trieste/Udine,
I-34100 Trieste, [ff]University of Trieste/Udine, I-33100 Udine, Italy
[53]University of Tsukuba, Tsukuba, Ibaraki 305, Japan
[54]Tufts University, Medford, Massachusetts 02155, USA
[55]University of Virginia, Charlottesville, VA 22906, USA
[56]Waseda University, Tokyo 169, Japan
[57]Wayne State University, Detroit, Michigan 48201, USA
[58]University of Wisconsin, Madison, Wisconsin 53706, USA
[59]Yale University, New Haven, Connecticut 06520, USA

Using data corresponding to 6.0 fb^{-1} of $p\bar{p}$ collisions at $\sqrt{s}$ = 1.96 TeV collected by the CDF II detector, we present a cross section measurement of top-quark pair production with an additional radiated photon, $t\bar{t}\gamma$. The events are selected by looking for a lepton (ℓ), a photon (γ), significant transverse momentum imbalance ($\not{E}_T$), large total transverse energy, and three or more jets, with at least one identified as containing a b quark (b). The $t\bar{t}\gamma$ sample requires the photon to have 10 GeV or more of transverse energy, and to be in the central region. Using an event selection optimized for the $t\bar{t}\gamma$ candidate sample we measure the production cross section of $t\bar{t}$ ($\sigma_{t\bar{t}}$), and the ratio of cross sections of the two samples. Control samples in the dilepton+photon and lepton+photon+$\not{E}_T$, channels are constructed to aid in decay product identification and background measurements. We observe 30 $t\bar{t}\gamma$ candidate events compared to the standard model expectation of 26.9 ± 3.4 events. We measure the $t\bar{t}\gamma$ cross section ($\sigma_{t\bar{t}\gamma}$) to be 0.18 ± 0.08 pb, and the ratio of $\sigma_{t\bar{t}\gamma}$ to $\sigma_{t\bar{t}}$ to be 0.024 ± 0.009. Assuming no $t\bar{t}\gamma$ production, we observe a probability of 0.0015 of the background events alone producing 30 events or more, corresponding to 3.0 standard deviations.

The standard model (SM) [1] of particle physics makes successful predictions of the production rates of physics processes that span many orders of magnitude. Data from $p\bar{p}$ collisions collected at the Tevatron have been used to verify many of these predictions [2]. As a test

[*]Deceased
[†]With visitors from [a]University of Massachusetts Amherst, Amherst, Massachusetts 01003, [b]Istituto Nazionale di Fisica Nucleare, Sezione di Cagliari, 09042 Monserrato (Cagliari), Italy, [c]University of California Irvine, Irvine, CA 92697, [d]University of California Santa Barbara, Santa Barbara, CA 93106 [e]University of California Santa Cruz, Santa Cruz, CA 95064, [f]CERN,CH-1211 Geneva, Switzerland, [g]Cornell University, Ithaca, NY 14853, [h]University of Cyprus, Nicosia CY-1678, Cyprus, [i]University College Dublin, Dublin 4, Ireland, [j]University of Fukui, Fukui City, Fukui Prefecture, Japan 910-0017, [k]Universidad Iberoamericana, Mexico D.F., Mexico, [l]Iowa State University, Ames, IA 50011, [m]University of Iowa, Iowa City, IA 52242, [n]Kinki University, Higashi-Osaka City, Japan 577-8502, [o]Kansas State University, Manhattan, KS 66506, [p]University of Manchester, Manchester M13

9PL, England, [q]Queen Mary, University of London, London, E1 4NS, England, [r]Muons, Inc., Batavia, IL 60510, [s]Nagasaki Institute of Applied Science, Nagasaki, Japan, [t]National Research Nuclear University, Moscow, Russia, [u]University of Notre Dame, Notre Dame, IN 46556, [v]Universidad de Oviedo, E-33007 Oviedo, Spain, [w]Texas Tech University, Lubbock, TX 79609, [x]Universidad Tecnica Federico Santa Maria, 110v Valparaiso, Chile, [y]Yarmouk University, Irbid 211-63, Jordan, [gg]On leave from J. Stefan Institute, Ljubljana, Slovenia,

of the SM, we measure the ratio of production cross sections of $t\bar{t}\gamma$ to $t\bar{t}$. The ratio allows for the cancellation of systematic effects, and is a more sensitive test of the SM than the measurement of the production cross section of $t\bar{t}\gamma$ alone. While current data is not sufficient to study them in detail, the $t\bar{t}\gamma$ coupling parameters are sensitive to some new physics models [3], and will be better measured in the future.

Top quarks are dominantly produced in pairs, with both top quarks decaying to a W boson and a b quark nearly 100% of the time. Their decays are classified as dileptonic if both W bosons decay to leptons, semileptonic if only one W boson decays to leptons, and hadronic if neither W boson decays to leptons. Selection for the $t\bar{t}\gamma$ events in a semileptonic channel (including τ leptonic decays) was performed using 6.0 fb^{-1} of integrated luminosity from $p\bar{p}$ collisions at $\sqrt{s} = 1.96$ TeV collected using the CDF II detector [4]. In order to isolate non-hadronic $t\bar{t}\gamma$ production, we require: a high-transverse-momentum (p_T) [5] lepton (ℓ) identifed as either an electron (e) or a muon (μ), a photon (γ), a b-tagged jet (b), missing transverse energy ($\not{E}_T$), large total transverse energy (H_T), and three or more jets. With these selection criteria, $t\bar{t}\gamma$ dominates SM predictions [6]. The total transverse energy, H_T, is the scalar sum of the transverse energy of electrons, muons, jets, photons, and $\not{E}_T$ identified in the event. Furthermore, we select top-quark pair production ($t\bar{t}$) events by using nearly the same selection as $t\bar{t}\gamma$, but without the photon requirement. Using similar event selection ensures that many systematic uncertainties cancel when we measure the cross section ratio of $t\bar{t}\gamma$ to $t\bar{t}$.

The semileptonic cross section of $t\bar{t}\gamma$ has been measured to be 0.15 ± 0.08 pb using data corresponding to an integrated luminosity of 1.9 fb^{-1} [6]. Using the branching ratio of W decays to leptons (0.324) [7], this corresponds to a production cross section of 0.34 ± 0.18 pb. The cross section of $t\bar{t}$ production is well-measured at 7.70 ± 0.52 pb [8]. However a measurement of both $t\bar{t}$ and $t\bar{t}\gamma$ cross sections with similar event selection has not been performed.

The CDF II detector is a cylindrically symmetric magnetic spectrometer designed to study $p\bar{p}$ collisions at the Fermilab Tevatron. Here we briefly describe the components relevant for this analysis. Tracking systems are used to measure the momenta of charged particles and to assist lepton identification. A multi-layer system of silicon strip detectors [9] which identifies tracks in the r - ϕ and r - z views [5], and the central outer tracker (COT) [10], are contained in a superconducting solenoid that generates a 1.4 T magnetic field. The COT is a 3.1 m long open-cell drift chamber capable of making up to 96 measurements of each charged particle in the pseudorapidity region $|\eta| < 1$ [5]. Sense wires are arranged in 8 alternating axial and $\pm 2°$ stereo superlayers with 12 wires each. For high-momentum tracks, the COT transverse momentum resolution is $\sigma_{pT}/p_T^2 \simeq 0.0015$ GeV^{-1}.

Segmented calorimeters with towers arranged in a projective geometry, each tower consisting of an electromag-

netic and a hadronic compartment [11], cover the region $|\eta| < 3.6$. In this analysis we select photons and electrons from the central region, $|\eta| \lesssim 1.0$, where the central electromagnetic shower system (CES) makes profile measurements at shower maximum with finer spatial resolution than the calorimeter. Electrons are reconstructed in the central electromagnetic calorimeter (CEM) with an E_T [5] resolution of $\sigma(E_T)/E_T \simeq 13.5\%/\sqrt{E_T/\text{GeV}} \oplus 1.7\%$. Jets are identified using the hadronic and electromagnetic calorimeter using a cone in $\eta - \phi$ space of radius $R = \sqrt{(\Delta\phi)^2 + (\Delta\eta)^2} = 0.4$. The jet energy resolution is approximately $\sigma \simeq 0.1 \times E_T(\text{GeV}) + 1$ GeV [12] (i.e. 2.5 GeV for a 15 GeV jet).

Jets containing a hadron with a b quark (b hadrons) are identified by exploiting the long b-hadron lifetime (c$\tau_b \approx$450 μm). The tracks originating from the resulting displaced vertex are used by the SECVTX [13] algorithm to identify the b hadron. The algorithm works in the region $|\eta| < 2$, defined by the silicon system coverage. Jets that are identified as coming from b hadrons are said to be b-tagged.

Muons (μ) are identified using the central muon (CMU), the central muon upgrade (CMP), and the central muon extension (CMX) systems [14], which cover the detector region $|\eta| < 1$.

Luminosity is measured using Čerenkov luminosity counters in the range $3.7 < |\eta| < 4.7$. The uncertainty in the luminosity has been estimated to be 6%, where 4.4% comes from the acceptance and operation of the luminosity monitor, and 4% comes from the uncertainty on the inelastic cross section of $p\bar{p}$ [15].

A three-level online event selection system (trigger) [4] selects events with a high-p_T lepton in the central region. The trigger system selects electron candidates from clusters of energy in the central electromagnetic calorimeter. Electrons are distinguished from photons by requiring a COT track associated with the clusters. The muon trigger requires a COT track that extrapolates to a track segment ("stub") in the muon detectors.

A muon candidate passing our selection criteria must have: a well-measured track in the COT, energy deposited in the calorimeter consistent with minimum-ionization expectations, a muon stub in both the CMU and CMP, or in the CMX, consistent with the extrapolated COT track, and COT timing consistent with a track from a $p\bar{p}$ collision.

An electron candidate passing our selection criteria must have: a high-quality track with $p_T > 0.5\,E_T$, unless $E_T > 100$ GeV, in which case the p_T threshold is set to 25 GeV, a good transverse shower profile that matches the extrapolated track position, a lateral sharing of energy in the two calorimeter towers containing the electron shower consistent with that expected for an electromagnetic (EM) shower, and minimal leakage into the hadron calorimeter [16].

Photon candidates are required to have $E_T^\gamma >$10 GeV, no track with $p_T > 1$ GeV and at most one track with $p_T < 1$ GeV, pointing at the EM cluster, good profiles

in both transverse dimensions at shower maximum, and minimal leakage into the hadron calorimeter [16]. The detected tracks have a minimum p_T of 0.35 GeV due to the magnetic field curling up lower p_T particles. The photons are only reconstructed in the CEM and have $|\eta| < 1.0$.

To reduce background from photons or leptons that originate from decays of hadrons produced in jets, both the photon and the lepton in each event are required to be "isolated". The E_T deposited in the calorimeter towers in a cone in $\eta - \varphi$ space [5] of $R = 0.4$ around the photon or lepton position is summed, and the E_T due to the photon or lepton is subtracted. The remaining E_T is required to be less than 2.0 GeV + $0.02 \times$ (E_T - 20 GeV) for a photon, or less than 10% of the E_T for electrons or p_T for muons. In addition, for photons, the sum of the p_T of all tracks in the cone must be less than 2.0 GeV + $0.005 \times E_T$.

Missing transverse energy, $\not{E}_T$, is calculated from the observed calorimeter-tower energies in the region $|\eta| <$ 3.6 [17]. Corrections are then made to the $\not{E}_T$ for non-uniform calorimeter response [18] for jets with un-corrected $E_T > 15$ GeV and $\eta < 2$, and for muons with $p_T > 20$ GeV.

Events for the analysis are selected by requiring a central e or μ with $E_T^\ell > 20$ GeV originating less than 60 cm along the beam-line from the detector center and passing the criteria listed above. We further require events to have at least one of the following objects: a jet with $E_T^{jet} > 15$ GeV, $\not{E}_T > 20$ GeV, an additional lepton, or a central γ with $E_T > 10$ GeV.

The first measurement we perform is in the $t\bar{t}$ signal sample, which requires an event to contain: $\not{E}_T >$ 20 GeV, a lepton, a b-tagged jet, $H_T > 200$ GeV, $N_{jets} \geq$ 3 [19] (including the b-tagged jet), and transverse mass of the lepton and $\not{E}_T$ to be greater than 20 GeV for the electron channel, and 10 GeV for the muon channel. Transverse mass for the $\not{E}_T$ and lepton is defined as: $\sqrt{2(E_{\ell,T} \times \not{E}_T - E_{\ell,x} \times \not{E}_{Tx} - E_{\ell,y} \times \not{E}_{Ty})}$. The selection criteria is inclusive, so if an event contains an additional lepton or a photon it is also accepted as a signal event. The highest-p_T lepton determines if the event is an electron or muon event.

Events in the $t\bar{t}\gamma$ signal sample are selected by requiring $\not{E}_T > 20$ GeV, a lepton, a b-tagged jet, $H_T >$ 200 GeV, $N_{jets} \geq 3$ (including the b-tagged jet.), and a photon with $E_T > 10$ GeV. For all photons we require the χ^2 of the CES shower profile be less than 20. To further suppress backgrounds, photons with E_T between 10 and 25 GeV must have a χ^2 of the CES shower profile less than 6; we discuss how χ^2 is calculated below. Similar to the $t\bar{t}$ analysis, the selection is inclusive. The selection criteria are identical to the previous $t\bar{t}\gamma$ cross section measurement [6], with the exception of the low-E_T photon χ^2 requirements.

The primary difference between the $t\bar{t}$ and $t\bar{t}\gamma$ selection, other than the photon selection, is the requirement of a transverse mass selection for $t\bar{t}$. In the $t\bar{t}$ selection, the low-transverse-mass region is not well-modeled with background estimation methods. The $t\bar{t}\gamma$ sample does not suffer from this deficiency, and we do not use the transverse mass selection criterion to keep acceptance of signal events high, this behavior is also seen in the $\ell\gamma\not{E}_T$ control sample described below.

Control samples are identified by selecting events with a lepton, a photon, and $\not{E}_T > 20$ GeV ($\ell\gamma\not{E}_T$), or two oppositely charged same-flavor central leptons, a photon, and a three-body mass consistent with the Z boson ($\ell\ell\gamma$). These control samples are used to define the above CES χ^2 selection for photons.

The χ^2 value of photons is based on the lateral shower shapes observed in the CES compared to that predicted from a sample of test-beam electrons. Using the control samples we identify an additional selection criterion on photons [20].It should be noted that the $t\bar{t}\gamma$ sample contains 30 events and is a subset of the 8276 events in the $\ell\gamma\not{E}_T$ sample. The $\ell\ell\gamma$ sample contains 1344 events. While the samples are not independent, optimizing photon identification selection criteria using the $\ell\gamma\not{E}_T$ sample should be minimally affected by the presence of $t\bar{t}\gamma$ events.

The dominant SM sources of events with a lepton, photon, and significant $\not{E}_T$, not including particle misidentifications, are $t\bar{t}\gamma$ production and $W\gamma$+heavy flavor (HF), in which a W boson decays leptonically ($\ell\nu$) and a photon is radiated from an initial-state or final-state quark, the W boson, or a charged final-state lepton [21]. In this paper, HF includes: $c\bar{c}$, $b\bar{b}$, and c. Similarly, for events in the $t\bar{t}$ selection, the dominant source of events is due to $t\bar{t}$ production and W+HF production.

The production of $t\bar{t}\gamma$ events with semileptonic and dileptonic decays, as well as the SM background of single-top events and associated production of a $W\gamma$+HF is estimated from leading-order (LO) matrix-element Monte Carlo simulations (MC) event generator MAD-GRAPH [22]. Events for all production and decays of $t\bar{t}$, WW, WZ, and ZZ signals are generated with PYTHIA [23]. The production of W+HF, as well as $Z+b\bar{b}$, and $Z \rightarrow \tau\tau$ decays are generated with ALPGEN [24]. Then the events are processed with the same reconstruction and analysis codes used for the data. Backgrounds from ZZ are estimated to be negligible to the $t\bar{t}\gamma$ signature.

Initial state radiation is simulated by the PYTHIA shower Monte Carlo simulation code tuned so as to re-produce the underlying event [25]. All of the generated samples are then passed through a full simulation of the detector, then reconstructed with the same reconstruction code used for the data.

The expected contributions from $t\bar{t}$, $W + HF$, single-top, $Z + b\bar{b}$, and $Z \rightarrow \tau\tau$ production to the $t\bar{t}$ search are given in Table I, and the expected contributions from $t\bar{t}\gamma$ and $W\gamma + HF$ production to the $t\bar{t}\gamma$ search are given in Table II. Additional contributions from misidentification backgrounds, described below, are also shown in the Ta-

TABLE I: Summary for predicted and observed events in the $t\bar{t}$ ($\ell \not{E}_T b + H_T > 200$ GeV + $N_{\text{jets}} \geq 3$) signal sample.

Predicted and Observed $t\bar{t}$ Events			
SM Source	$eb\not{E}_T$	$\mu b\not{E}_T$	$(e+\mu)b\not{E}_T$
$t\bar{t}$	1420 ± 180	1080 ± 140	2500 ± 330
WW	29 ± 4	22 ± 3	51 ± 7
WZ	8.6 ± 1.1	6.5 ± 0.9	15.1 ± 2.0
ZZ	1.3 ± 0.2	1.0 ± 0.1	2.3 ± 0.3
Wbb	203 ± 34	146 ± 24	348 ± 58
Wcc	127 ± 23	94 ± 17	221 ± 40
Wc	85 ± 13	61 ± 9	147 ± 23
Single top (s-ch.)	76 ± 10	59 ± 8	135 ± 18
Single top (t-ch.)	66 ± 9	50 ± 7	116 ± 16
$(Z \to \ell\ell)b\bar{b}$	31 ± 3	22 ± 2	53 ± 5
$Z \to \tau\tau$	6 ± 8	9 ± 8	14 ± 11
Mistags	358 ± 29	214 ± 17	572 ± 46
QCD	222 ± 38	20 ± 3	240 ± 40
Total Predicted	2630 ± 196	1790 ± 146	4420 ± 340
Observed	2720	1709	4429

bles. Figure 1 shows kinematic distributions for the $t\bar{t}$ sample, and Figs. 2 and 3 show distributions for events in the $t\bar{t}\gamma$ sample. There is good agreement between data and standard-model predictions. We show the data and background predictions combined for both electron and muon events; there is good agreement in both channels individually, as shown in [20].

High p_T photons are copiously produced in hadron jets initiated by a scattered quark or gluon. In the $t\bar{t}\gamma$ sample, the number of events in which a jet is misidentified
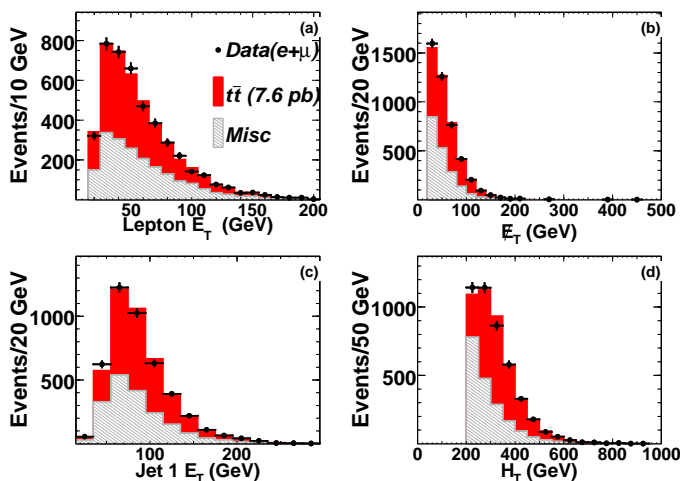

FIG. 1: The distributions for events in the $t\bar{t}$ sample (points) of a) the E_T of the lepton; b) the missing transverse energy $\not{E}_T$; c) the E_T of the highest E_T jet; and d) the total transverse energy H_T. The histograms show the expected SM contributions from top production ($t\bar{t}$), and miscellaneous backgrounds (Misc), which include: diboson production, single top, W+HF and Z+HF production as well as jets misidentified as leptons (QCD), and misidentified b tags.

as a photon (jet faking photon) is estimated by removing the isolation requirements on the photon. We fit the resulting isolation distribution using signal and background templates obtained from data. The signal template is constructed using electrons from $Z^0/\gamma^* \to ee$ events, and
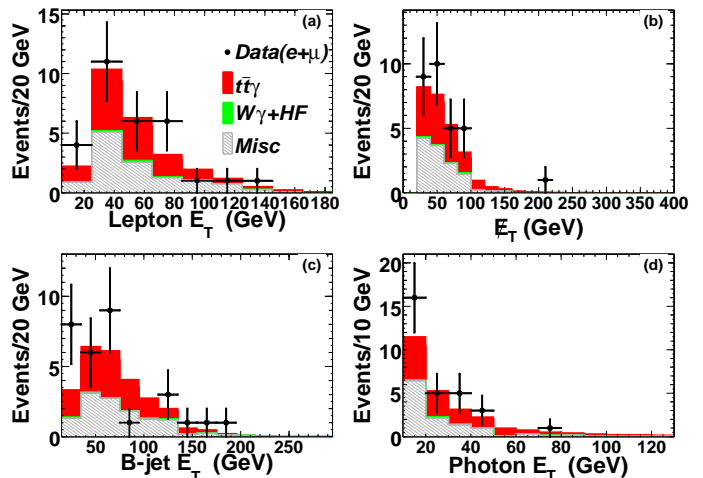

FIG. 2: The distributions for events in the $t\bar{t}\gamma$ sample (points) in a) the E_T of the lepton; b) the missing transverse energy, $\not{E}_T$; c) the E_T of the b jet; and d) the E_T of the photon. The histograms show the expected SM contributions from radiative top production ($t\bar{t}\gamma$), $W\gamma$ production with heavy flavor (HF), and miscellaneous backgrounds (Misc), which include: WW and WZ production as well as jets, τ leptons, electrons, and jets misidentified as photons, jets misidentified as leptons (QCD), and misidentified b tags.

TABLE II: Summary for $t\bar{t}\gamma$ ($\ell\gamma\not{E}_T b + H_T > 200$ GeV + $N_{\text{jets}} \geq 3$). Monte Carlo samples listed in the table are given as they were generated (e.g., WW was not generated with an associated photon.) Backgrounds from ZZ are found to be negligible.

| Predicted and Observed $t\bar{t}\gamma$ Candidate Events			
SM Source	$e\gamma b\not{E}_T$	$\mu\gamma b\not{E}_T$	$(e+\mu)\gamma b\not{E}_T$
$t\bar{t}\gamma(semilep)$	5.98 ± 1.10	5.21 ± 0.97	11.19 ± 2.04
$t\bar{t}\gamma(dilep.)$	1.47 ± 0.27	1.27 ± 0.24	2.74 ± 0.50
$Wc\gamma$	$0^{+0.07}_{-0}$	$0^{+0.07}_{-0}$	$0^{+0.09}_{-0}$
$Wcc\gamma$	$0^{+0.05}_{-0}$	0.05 ± 0.05	0.05 ± 0.07
$Wbb\gamma$	0.15 ± 0.07	0.06 ± 0.05	0.21 ± 0.08
WZ	0.05 ± 0.05	0.05 ± 0.05	0.09 ± 0.06
WW	0.06 ± 0.03	0.06 ± 0.03	0.11 ± 0.03
Single Top (s-chan)	0.09 ± 0.10	0 ± 0.10	0.09 ± 0.13
Single Top (t-chan)	0.14 ± 0.14	0.13 ± 0.14	0.27 ± 0.19
$\tau \to \gamma$ fake	0.20 ± 0.08	0.10 ± 0.05	0.29 ± 0.09
Jet faking γ	5.75 ± 1.76	1.79 ± 1.56	7.54 ± 2.53
Mistags	1.47 ± 0.37	1.02 ± 0.32	2.50 ± 0.51
QCD	0.38 ± 0.38	0.02 ± 0.02	0.40 ± 0.38
$ee\not{E}_T b, e\to\gamma$	0.94 ± 0.19	–	0.94 ± 0.19
$\mu e\not{E}_T b, e\to\gamma$	–	0.49 ± 0.11	0.49 ± 0.11
Total Predicted	16.7 ± 2.2	10.3 ± 1.9	26.9 ± 3.4
Observed	17	13	30
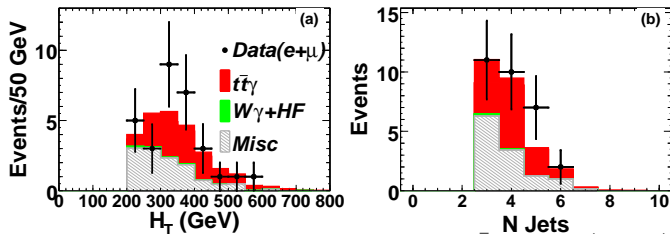
FIG. 3: The distributions for events in the $t\bar{t}\gamma$ sample (points) of a) the total transverse energy H_T, the sum of the transverse energies of the lepton, photon, jets and $\not{E}_T$, for the $t\bar{t}\gamma$ events; b) the total number of jets . The histograms show the expected SM contributions from radiative top-quark pair production ($t\bar{t}\gamma$), $W\gamma$ production with heavy flavor ($W\gamma$+HF), and miscellaneous backgrounds (Misc), which include: SM WW and WZ production as well as jets, τ leptons, electrons, and jets misidentified as photons, jets misidentified as leptons (QCD), and misidentified b tags.

a background template is made from a QCD enriched sample [20, 26].

The expected number of events in which an electron is misidentified as a photon in the $t\bar{t}\gamma$ signature is determined by measuring the electron E_T spectrum in the $\ell\not{E}_Tb+e+$large H_T, and ≥ 3 jets sample (events of this type are created from dileptonic, ee or $e\mu$, $t\bar{t}$ and diboson decays), and then multiplying by the probability that an electron is misidentified as a photon. The latter is measured in data using $Z^0/\gamma^* \rightarrow ee$ events that are misreconstructed as $Z^0/\gamma^* \rightarrow e\gamma$.

To estimate the number of b-tagged jets that are in reality mistagged light-quark jets (mistags), each jet in the $\ell\gamma\not{E}_T+ \geq 3$ jets and high-H_T sample is weighted by a mistag rate. The mistag rate per jet is measured using a large inclusive-jet sample. For the $t\bar{t}$ sample, a similar procedure is used. Each jet in the signal samples has a corresponding probability to be identified as a b-tagged jet. In all cases, however, the resulting prediction is overestimated because we count as mistags, events which have true heavy flavor jets (i.e. events due to $t\bar{t}$ events may be mistagged, but they will be accounted for in the MC). The fraction's denominator is computed by finding the total number of $\ell\gamma\not{E}_T \geq 3$ jets (or $t\bar{t}$ analogue) events. Its numerator is the difference between the denominator and the number of events in the sample with b-tagged jets predicted by MC simulations. The fraction is the amount of events that have no true heavy flavor content relative to the size of $\ell\gamma\not{E}_T \geq 3$ jets (or $t\bar{t}$ analogue) sample; it is used to scale our mistag estimate. This scaled background estimate removes events which contain actual heavy flavor content from the mistag total; the scale factor is nearly 60%.

The background due to events in which a jet is misidentified as a lepton (QCD) is estimated using "non-electrons". "Non-electrons" are jets which are kinematically similar to electrons, but which fail a pair of selection criteria normally passed by electrons (regardless of energy) such as: EM shower-shape, energy over mo-

mentum, or isolation. "Non-electrons" play the role of leptons in our model of the QCD background. The remaining object selection is unchanged. In each signature, a template of signal events in data with $\not{E}_T < 20$ GeV are fit to the sum of MC backgrounds and a scaled "non-electron" signal. The QCD background is the sum of the scaled "non-electron" events in the $\not{E}_T > 20$ GeV region expected from the fit.

To avoid double counting, the total background yields are corrected by removing the predicted number of events with two objects misidentified. Each of the aforementioned data-driven background estimates accounts for a background process where one object in the event is misidentified. Events with two misidentified objects would be counted in a pair of background estimates. In the $t\bar{t}$ sample, double counting is accounted for by removing the QCD background from the mistagging background, and vice versa.

The background from tau leptons, which decay to hadrons, which decay to photons is a background estimated from the $t\bar{t}$ MC sample by selecting $\tau \rightarrow hadrons \rightarrow \gamma$ events using MC information.

The $t\bar{t}$ event detection efficiency and acceptance are calculated using the MC simulation which has all decays of $t\bar{t}$. The uncertainty on the $t\bar{t}$ cross section is dominated by systematic uncertainties. The $t\bar{t}\gamma$ event detection efficiency and acceptance are calculated using both semileptonic, and dileptonic decays of the pair of top quarks in the decay. The total $t\bar{t}\gamma$ cross section is then calculated assuming that $t\bar{t}\gamma$ has the same branching ratio to semileptonic and dileptonic decays as $t\bar{t}$ pair production. The uncertainty in the $t\bar{t}\gamma$ cross section measurement is dominated by statistics.

Systematic uncertainties have been calculated by varying detector efficiencies and resolutions within known uncertainties and evaluating the change in our measurements. These uncertainties are added in quadrature when independent, and summed when positively (or negatively) correlated. The largest uncertainties, given in descending order, are due to luminosity, b-hadron tagging efficiencies and, for the $t\bar{t}\gamma$ sample, photon identification.

We observe 30 $t\bar{t}\gamma$ candidate events compared to an expectation of 26.9 ± 3.4. We observe 4429 $t\bar{t}$ events, with an expectation of 4420 ± 340. Assuming the difference between the non-$t\bar{t}$ background estimate and the number of observed events is due to SM $t\bar{t}$ production, we measure the $t\bar{t}$ cross section to be 7.62 ± 0.20 (stat) ± 0.68 (sys) ± 0.46 (lum) pb. The theoretical production cross section of $t\bar{t}$ at the Tevatron is $7.08^{+0.00}_{-0.32}\,^{+0.36}_{-0.27}$ pb [27]. The first uncertainty comes from scale uncertainty around $\mu = m_{top}$, and the second is due to parton distribution function uncertainties.

If one assumes that $t\bar{t}\gamma$ is not allowed in the SM, and there are no new physics processes contributing to this sample, the probability that the background events alone will produce 30 or more events is 0.0015 (3.0 standard deviations). This is the first experimental evidence for $t\bar{t}\gamma$ production. Assuming the difference between the back-

ground estimate and the number of observed events is due to SM $t\bar{t}\gamma$ production, we measure the $t\bar{t}\gamma$ cross section to be 0.18 ± 0.07 (stat) ±0.04 (sys) ±0.01 (lum) pb. The $t\bar{t}\gamma$ event detection efficiency and acceptance are calculated using the MC sample requiring at least one W boson decaying leptonically. The acceptance times efficiency, using both semileptonic and dileptonic modes, for this $t\bar{t}\gamma$ signal is 0.015 ± 0.002. The uncertainty on the measured cross section is dominated by the statistical uncertainties associated with the small number of events observed. A theoretical value for the non-hadronic decays of $t\bar{t}\gamma$ (sum of all three lepton flavors) cross section $\sigma_{t\bar{t}\gamma} = 0.071 \pm 0.011$ pb is obtained from leading order (LO) MADGRAPH semileptonic cross section $\sigma_{t\bar{t}\gamma} = 0.0726$ pb multiplied by a K-factor to find the next to leading order (NLO); K-factor $= \sigma_{NLO}/\sigma_{LO} = 0.977$ [28]. The next to leading order theoretical total cross section for $t\bar{t}\gamma$ is thus $\sigma_{t\bar{t}\gamma}^{total} = 0.17 \pm 0.03$ pb.

The ratio between the production cross sections of $t\bar{t}\gamma$ and $t\bar{t}$ is measured to be $\Re = 0.024 \pm 0.009$ which agrees with the SM prediction of $\Re = 0.024 \pm0.005$, obtained from theoretical predictions of the cross sections of $t\bar{t}\gamma$ and $t\bar{t}$. When measuring $\Re$ many of the systematic uncertainties nearly cancel, such as those due to: lepton identification, b hadron identification, jet energy scale, and luminosity uncertainties. However, other systematic uncertainties do not cancel out completely such as: QCD systematic uncertainties, and photon identification and acceptance uncertainties. The total systematic uncertainties combine to less than 10% however the statistical uncertainty is the dominant contribution to the total uncertainty.

In conclusion, we have performed a search for $t\bar{t}\gamma$,

which is the dominant standard model process that produces the event signature of lepton + photon + $\not{E}_T$ + b-jets with large total transverse energy and $N_{jets} \geq 3$. We find that the numbers of events observed are consistent with SM predictions. We obtain a $t\bar{t}\gamma$ cross section $\sigma_{t\bar{t}\gamma} = 0.18 \pm 0.08$ pb, and the ratio of production cross sections of $t\bar{t}\gamma$ to $t\bar{t} = 0.024 \pm 0.009$.

[1] S.L. Glashow, Nucl. Phys. **22** 588, (1961); S. Weinberg, Phys. Rev. Lett. **19** 1264, (1967); A. Salam, Proc. 8th Nobel Symposium, Stockholm, (1979).
[2] S. Rolli, Proceeding of the HCP 2010 conference, Toronto, Canada, (2010).
[3] U. Baur, M. Buice, and L. H. Orr, Phys. Rev. D. **64**, 094019, (2001).
[4] D. Acosta et al. (CDF Collaboration), Phys. Rev. D **71**, 032001 (2005).
[5] The CDF coordinate system of r, φ, and z is cylindrical, with the z-axis along the proton beam. The pseudorapidity is $\eta = -\ln(\tan(\theta/2))$. Transverse momentum and energy are defined as $p_T = p\sin\theta$ and $E_T = E\sin\theta$, respectively. We use the convention that "momentum" refers to pc and "mass" to mc^2. The coordinate y points up and down, and x completes the right-handed system.
[6] T. Aaltonen et al. (CDF Collaboration), Phys. Rev. D **80**, 011102(R) (2009).
[7] K. Nakamura et al. (Particle Data Group), J. Phys. G 37, 075021 (2010).
[8] T. Aaltonen et al. (CDF Collaboration), Phys. Rev. Lett **105**, 012001 (2010).
[9] A. Sill et al., Nucl. Methods A **447**, 1 (2000); A.

Affolder et al., Nucl. Instrum. Methods A **453**, 84 (2000); C.S. Hill, Nucl. Instrum. Methods A **530**, 1 (2000).
[10] A. Affolder et al., Nucl. Instrum. Methods A **526**, 249 (2004).
[11] S. Kuhlmann et al., Nucl. Instrum. Methods A **518**, 39, (2004);
S. Bertolucci et al., Nucl. Instrum. Methods A **267**, 301 (1988).
[12] F. Abe et al., (CDF Collaboration) Phys. Rev. Lett. **68**, 1004 (1992).
[13] D. Acosta et al. (CDF Collaboration) Phys. Rev. D, **71**, 052003 (2005).
[14] The CMU consists of a central barrel of gas proportional wire chambers in the region $|\eta| < 0.6$; the CMP system consists of chambers after an additional meter of steel, also for $|\eta| < 0.6$. The CMX chambers cover $0.6 < |\eta| < 1.0$.
[15] D. Acosta et al. (CDF Collaboration), Nucl. Instrum. Methods Phys. Res., Sect. A **494**, 57 (2002).
[16] The fraction of electromagnetic energy allowed to leak into the hadron compartment E_{had}/E_{em} must be less than $0.055+0.00045 \times E_{em}(GeV)$ for central electrons, less than 0.05 for electrons in the end-plug calorimeters,

less than max[0.125, 0.055+0.00045×E_{em}(GeV)] for photons.

[17] Missing E_T ($\vec{\not{E}}_T$) is defined by $\vec{\not{E}}_T = -\sum_i E_T^i \hat{n}_i$, where i is the calorimeter tower number for $|\eta| < 3.6$, and $\hat{n}_i$ is a unit vector perpendicular to the beam axis and pointing at the ith tower. We correct $\vec{\not{E}}_T$ for jets and muons. We define the magnitude $\not{E}_T = |\vec{\not{E}}_T|$.

[18] A. Bhatti *et al.*, Nucl. Instrum. Methods Phys. Res., Sect. A 566, 375 (2006).

[19] A. Abulencia *et al.* (CDF Collaboration), Phys. Rev. D., **73** 112006 (2006).

[20] B. Auerbach, Ph. D Thesis, Yale University, FERMILAB-THESIS-2011-04, 2011.

[21] D. Acosta *et al.* (CDF Collaboration), Phys. Rev. Lett. **94**, 041803 (2005).

[22] T. Stelzer and W. F. Long, Comput. Phys. Commun. **81**, 357 (1994); F. Maltoni and T. Stelzer, J. High Energy Phys. **302**, 27 (2003).

[23] T. Sjöstrand, Comput. Phys. Commun. **82** (1994) 74; S. Mrenna, Comput. Phys. Commun. **101** (1997) 232.

[24] F. Carnavaglios *et al.*, Nucl. Phys. **B539**, 215 (1999).

[25] R. Field and R. C. Group, arXiv, hep-ph/0510198v1.

[26] A. Abulencia (CDF Collaboration) Phys. Rev. Lett. **97**, 031801 (2006); A. Abulencia (CDF Collaboration) Phys. Rev. D **75**, 112001 (2007); A. Loginov, Ph.D thesis, Institute for Theoretical and Experimental Physics, Moscow, Russia FERMILAB-THESIS-2006-48, 2006.

[27] N. Kidonakis, arXiv, hep-ph/1008 2460.

[28] D. Peng-Fei *et al.*, arXiv, hep-ph/0907 1324.